Proceedings Volume 2, 2011

Earthquake Geology and Archaeology: Science, Society and Critical Facilities

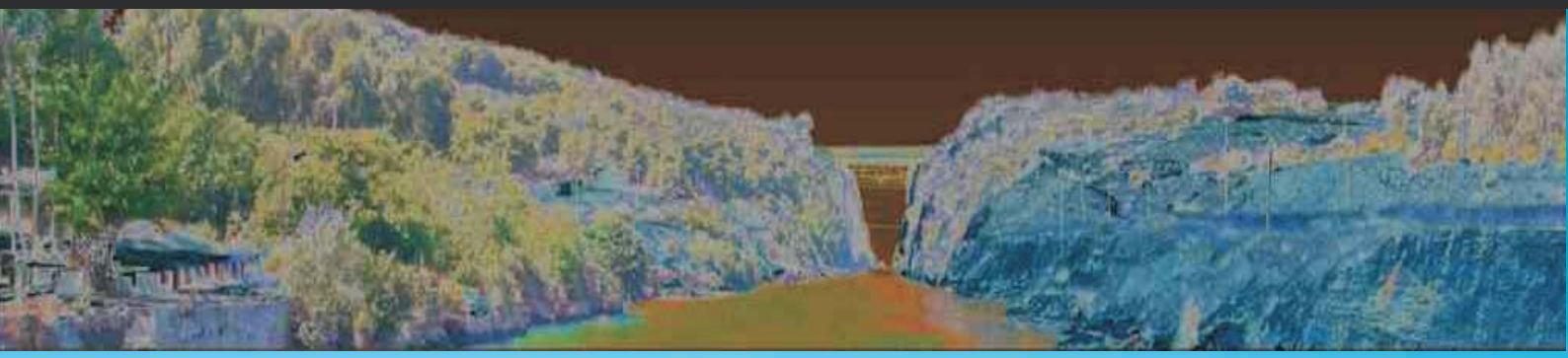

Editors

C. Grützner, R. Pérez-López, T. Fernández Steeger, I. Papanikolaou
K. Reicherter, P.G. Silva, and A. Vött

PROCEEDINGS

2nd INQUA-IGCP 567 International Workshop on Active Tectonics, Earthquake Geology, Archaeology and Engineering

19-24 September 2011
Corinth (Greece)

ISBN: 978-960-466-093-3

THE SPARTA FAULT, SOUTHERN GREECE: TECTONIC GEOMORPHOLOGY, SEISMIC HAZARD MAPPING AND CONDITIONAL PROBABILITIES

Papanikolaou Ioannis D. (1,2), Gerald Roberts (2), Georgios Deligiannakis (1,3), Athina Sakellariou (1), Emmanuel Vassilakis (3)

(1) Mineralogy-Geology Laboratory, Department of Earth and Atmoshperic Sciences, Agricultural University of Athens, Iera Odos 75, 118-55, Athens, Greece
(2) AON Benfield UCL Hazard Research Centre, Department of Earth Sciences Birkbeck College and University College London, WC 1E 6BT,London UK, Email: (i.papanikolaou@ucl.ac.uk)
(3) Laboratory of Natural Hazards, Faculty of Geology and Geoenvironment, National and Kapodistrian University of Athens, Panepistimioupolis, 15784, Athens, Greece

Abstract (The Sparta fault, southern Greece: Tectonic geomorphology, seismic hazard mapping and conditional probabilities): *The Sparta Fault system is a major structure approximately 64km long that bounds the eastern flanks of the Taygetos Mountain front (2.400m) and shapes the present-day Sparta basin. This fault is examined and described in terms of its geometry, segmentation, drainage pattern and postglacial finite throw, emphasizing also how these parameters vary along strike the fault. Based on fault throw-rates and the bedrock geology, geological data can offer both a qualitative and quantitative approach of the expected hazard distribution. This is achieved by the construction of a seismic hazard map based on fault throw-rates that shows the number of times a locality receives enough energy to shake at a certain intensity value, extracting a locality specific long-term earthquake recurrence record. The Sparta fault was activated in 464 B.C., devastating the city of Sparta. Since no other major earthquake has been generated by this system since 464 B.C., a future event could be imminent. As a result, not only time-independent but also time-dependent probabilities, which follow the concept of the seismic cycle, have been calculated for the city of Sparta.*

Key words*: Lakonia, slip-rates, time-dependent probabilities, Taygetos,*

INTRODUCTION

In 464 B.C. a large earthquake devastated the city of Sparta (~20000 fatalities), causing great social unrest (Papazachos and Papazachou, 1997). This event is regarded as the oldest well-defined event in the Hellenic historical record (Papazachos and Papazachou, 1997). However, the area is characterized by low seismicity over the last 25 centuries (Papanastassiou, 1999) and no other major event has occurred in the town of Sparta since 464 B.C, suggesting that a future event could be imminent. This is also supported by cosmogenic dating techniques applied on the Sparta bedrock scarp showing that this fault ruptured repeatedly (six times over the last 13kyrs), with time intervals ranging from 500-4500yrs (Benedetti et al., 2002). This fault is studied in detail based on its postglacial scarp, the analysis of the drainage network and the major catchments that are influenced by footwall uplift.

THE SPARTA FAULT SYSTEM

The Sparta fault system (Fig. 1), bounds the eastern part of the Taygetos Mt (2.407m) and shapes the western boundary of the Sparta basin (Fig.2). It trends NNW-SSE and has a length of 64km. Its southern tip is located close to the Gerakari catchment approximately 2-3km SW from the Potamia village, whereas its northern tip towards the Alfios river, a couple of km westwards from the Kamaritsa village in the Megalopolis basin. Two major faults are traced within this structure (Fig.1). The northern segment is about 14 km long and characterized by lower slip-rates. On the other hand, the southern segment is 50km long and leaves the most impressive imprint in the topography showing sings of recent intense activity. The southern segment can be divided into two patches that in the past were probably two individual structures that are now hard-linked. This fault exhibits an impressive postglacial scarp that can be traced for many km (Fig.3). In particular, from the village of Anogia up to the area of Mystras, it is continuous and has an 8-12m high scarp (Fig.4).

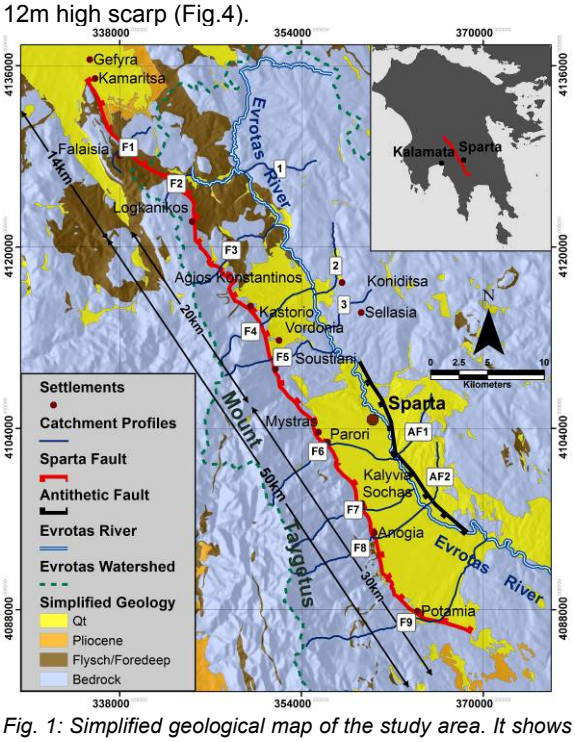

Fig. 1: Simplified geological map of the study area. It shows the segmentation pattern as well as the localities of the studied catchments profiles.

Fig.2: Distant view of the Sparta fault. It uplifts the Taygetos Mt on its footwall and shapes the basin of Sparta towards its hanging wall.

Fig.3: View of the post-glacial scarp of the Sparta fault in the Kalyvia-Sochas locality.

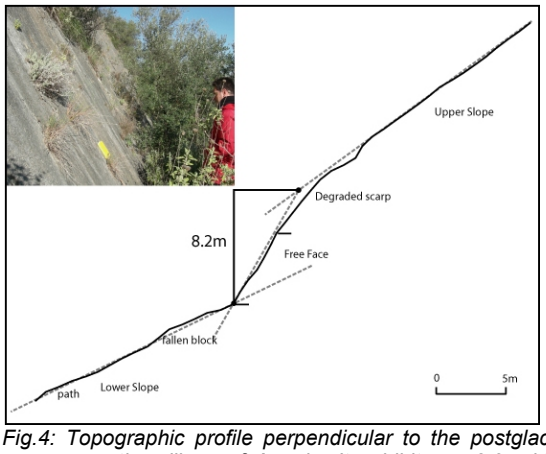

Fig.4: Topographic profile perpendicular to the postglacial scarp near the village of Anogia. It exhibits an 8.2m high scarp.

TECTONIC GEOMORPHOLOGICAL ANALYSIS; CATCHMENTS AND TECTONIC UPLIFT

The Evrotas river flows through the Sparta Basin, parallel to the Sparta Fault, trending NNW-SSE, while the secondary branches of this fluvial system consist of transient rivers which flow perpendicular to the main structure, indicating a strong tectonic influence to the drainage pattern. The combination of fault parallel and fault perpendicular flow is characteristic of active normal faulting settings.

Kirby & Whipple (2003) demonstrated that tectonically unperturbed "equilibrium" fluvial long profiles are typically smooth and concave-up. However, upland rivers are also sensitive to along-stream variations in differential uplift (potentially leading to changes in the profile concavity or steepness index) and also to changes in uplift rate through time. Whittaker et al. (2008) showed that rivers with drainage areas greater than 10km^2 and crossing faults that have undergone an increase in throw rate within the last 1Myrs have significant long-profile convexities. They also established that this relationship holds for throw rate variation along strike the same fault segment, as well as between faults. Moreover, Boulton & Whittaker (2009) suggested that rivers crossing active faults are undergoing a transient response to ongoing tectonic uplift and this interpretation is supported by typical signals of transience such as gorge formation and hill slope rejuvenation within the convex reach.

Nine fluvial long profiles of the transient rivers crossing different segments of the Sparta fault were studied in order to examine the longitudinal convexity and its variation along strike. Such profiles were also compared to the longitudinal profiles of rivers that are not influenced by any fault. Furthermore, in order to examine the transience of the streams across the Sparta fault, cross sections perpendicular to the river flow in the headwaters and within the downstream convex reach were analyzed.

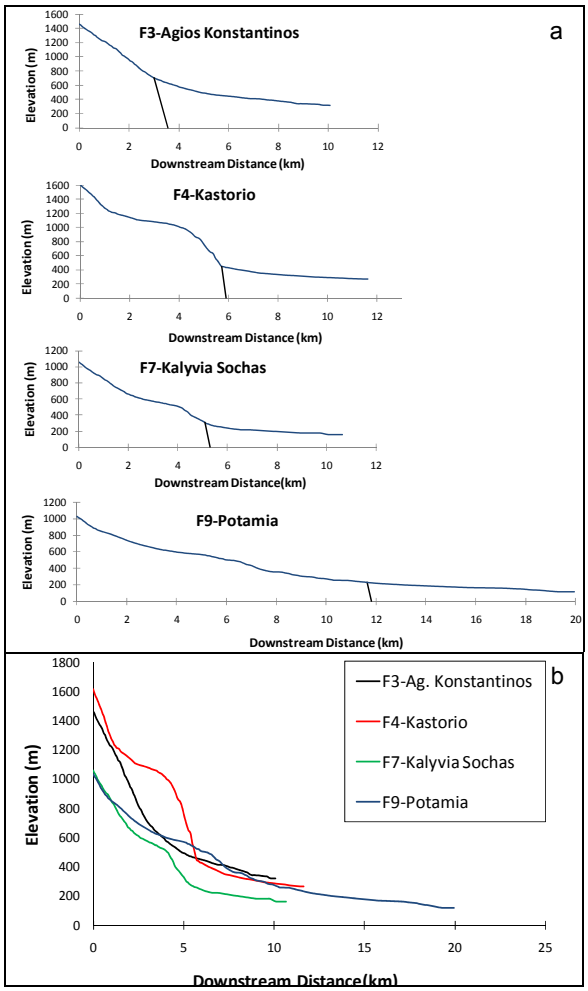

Fig.5: a) Long profiles of catchments crossing perpendicular the Sparta Fault. Locality names are shown geographically in Fig.1. b) Comparison of long profiles in the same graph of the above catchments showing significant differences in longitudinal convexities along strike the faults.

While river long profile convexities can lead to the observation of the ongoing tectonic uplift, differential erosion of geological formations may also cause the same pattern. Thus, in order to exclude the latter phenomena and emphasize the tectonic uplift, the rivers to be examined must fulfill some restrictions. Whittaker, et al. (2008) suggest that the selected rivers should discharge a drainage basin larger than 10km^2 above fault and the upstream length should be at least 5km. These restrictions are applicable in the south and central segments of Sparta fault. However, in the northern segment of Sparta fault the streams are not long enough to fulfill these criteria, due to the proximity of the watershed of Evrotas Basin to the SW segment of the fault.

Catchments crossing the North, Central and South parts of the Sparta Fault were grouped and studied separately. Qualitative analysis of long profiles showed a significant difference in longitudinal convexity between the Central and both the South and North parts of the fault, leading to the conclusion of varying uplift rate along strike. A convex reach of 205m height in Potamia catchment long profile (southeast part of the Sparta Fault) can be observed although it seems to have propagated upstream in relation to the fault. This could happen as the channel successively adjusts to the imposed uplift field (Whipple & Tucker, 2002). Moreover, Kalyvia Sochas fan deposits were extensively examined by Pope et al. (2003). Kalyvia Sochas catchment long profile revealed a convex reach of 246m height, which is in contact with the Sparta fault, in contrast to Potamia catchment's convex reach. Agios Konstantinos catchment seems to have a concave-up channel profile, possibly indicating a constant slip rate (Whittaker, et al. 2008). On the other hand, towards the central part of the Sparta fault, were no fan deposits and talus cones appear and the finite throw is smaller, the Kastorio catchment's convex reach height outreaches 590m, as measured from the fault (Fig. 5a,5b).

In addition, the normalized steepness index, k_{sn}, using a reference concavity of 0.45, was calculated for six catchments crossing all Sparta fault parts, as well as for the two catchments crossing the antithetic structure and two catchments that cross no fault (localities shown in Figure 1). The k_{sn} rates for the catchments closer to the tips of the Sparta fault (F3-Agios Konstantinos and F9-Potamia) were 81 and 82.7 respectively, while in the central part the steepness rates are higher and vary from 98.5 to 114 ($98.5<k_{sn}<114$). Along-strike variations of this scale show that the central part of the Sparta Fault appears to have undergone an increase in relative uplift rate compared to the other two parts. Moreover, the height of the convex reach in Kastorio channel profile could also indicate that the Sparta Fault has been tectonically active as one hard-linked structure only for the last couple of hundred of thousand years. Prior to this linkage there were two separate segments with different lengths and displacements. This can explain the absence of Upper Pleistocene sediments and alluvial fans and the smaller finite throw of the Kastorio-Soustiani segment.

SEISMIC HAZARD MAP FROM GEOLOGICAL FAULT SLIP-RATE DATA

Methodology

Fault throw-rates are firstly converted into earthquake frequencies, assuming that each fault ruptures in "floating" earthquakes, which are distributed around a mean magnitude of fixed size. Then, this information is turned into a hazard map after using: i) empirical relationships between coseismic slip values, rupture lengths and earthquake magnitudes, and ii) empirical relationships between earthquake magnitudes and intensity distributions (see Papanikolaou 2003 and Roberts et al., 2004). The final product is a high spatial resolution seismic hazard map showing how many times each location has been shaken at a certain intensity value (e.g. intensity IX) over a fixed time period (e.g. since the last glaciation), which can be easily transformed into a map of recurrence intervals.

Empirical relationships

For the Greek territory, magnitude-intensity laws and attenuation relationships are extracted from statistical elaboration of historical and instrumental data. However, there are significant differences between published data regarding the relationship between Magnitude, epicentral intensity and its attenuation with distance (Papaioannou 1984, Theodoulidis 1991, Papazachos & Papaioannou 1997). More importantly, for an M=7.0 earthquake, that a structure similar to the Sparta fault is able to generate (Wells & Coppersmith, 1994; Benedetti et al., 2002), only Theodoulidis's (1991) equations result in an epicentral intensity X, as has been clearly demonstrated by the Sparta 464 B.C. macroseismic field (Papazachos & Papaioannou 1997). Theodoulidis (1991) proposes that an earthquake with epicentral intensity X has a mean radius of 6-7km for the X isoseismal and a mean radius of 16-18km, for the isoseismal IX depending of which variable is used.

Results

Figure 6 shows how many times a locality receives enough energy to shake at intensities ≥IX in 15±3kyrs. Highest hazard is observed, as expected, towards the hangingwall centre of the Sparta fault and diminishes towards the tips, following the slip-rate variability. The town of Sparta lies closer to the hangingwall centre and is founded on Quaternary sediments, whereas surrounding villages are founded on alluvial fans and triangular facets. Therefore, it will receive enough energy to shake at intensity X, 8 or 9 times (lies on the boundary) over 15±3kyrs. The latter implies that it experiences a destructive event similar to the 464 B.C. approximately every 1792±458yrs years.

TIME INDEPENDENT AND TIME DEPENDENT PROBABILITIES FOR THE TOWN OF SPARTA

Following the results above a time-independent probability of 1,66% over the next 30 years and 2,75% over the next 50 years is calculated for the

town of Sparta. A considerably higher time-dependent probability of 2,14% over the next 30 years and 3,55% over the next 50 years has been calculated. The time dependent probability follows the seismic cycle concept (WGCEP 2002) and exhibits higher values because the elapsed time since the last event (2475yrs) has exceeded the mean recurrence interval (1792±458yrs). However, due to the irregularity of earthquake time intervals of the Sparta fault (Benedetti et al. 2002) and the introduction of a high sigma value (σ=0.64) this difference is noteworthy, but not substantial.

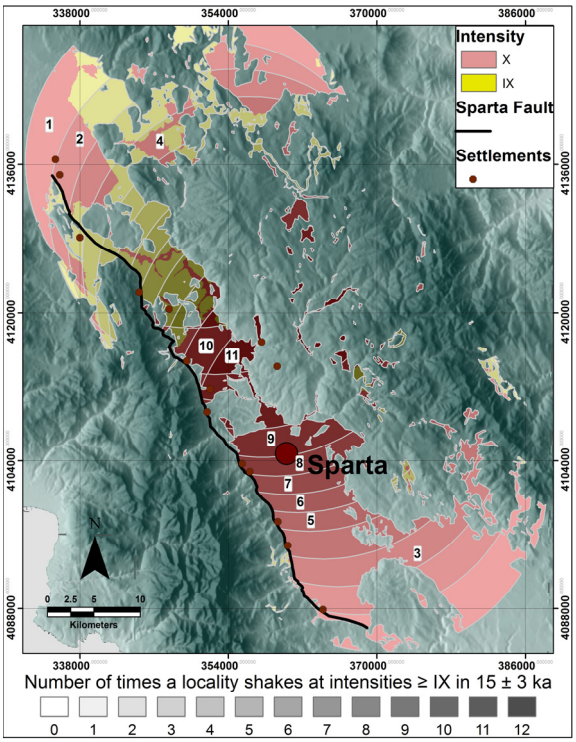

Fig.6: Seismic hazard map for the Sparta Basin, showing how many times a locality receives enough energy to shake at intensities ≥IX in 15±3kyrs, after considering the bedrock geology and assuming a circular pattern of energy release, with a 18 km radius of isoseismal IX.

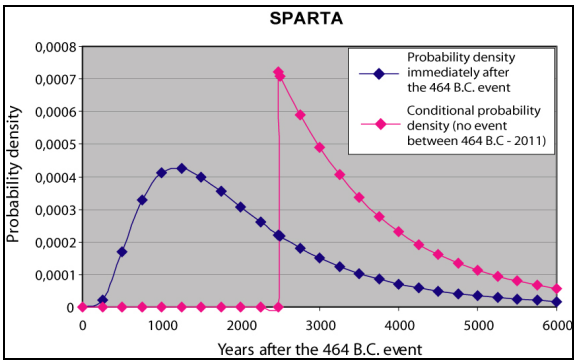

Fig. 7: Diagram showing the probability density for the town of Sparta immediately after the 464 B.C. event and the conditional probability density considering that no event occurred since 2011. A sigma value of 0.64 is used.

Acknowledgements: The Institution of State Scholarships of Greece is thanked for support.

References

Benedetti, L, et al. (2002). Post-glacial slip history of the Sparta fault (Greece) determined by ^{36}Cl cosmogenic dating: Evidence for non-periodic earthquakes. Geophys. Res. Letters 29, 10.1029/2001GL014510.

Boulton, S.J., Whittaker, A.C., (2009). Quantifying the slip rates, spatial distribution and evolution of active normal faults from geomorphic analysis: Field examples from an oblique-extensional graben, southern Turkey. Geomorphology 104, 299-316.

Kirby, E., Whipple K.X., (2003). Distribution of active rock uplift along the eastern margin of the Tibetan Plateau: Inferences from bedrock channel longitudinal profiles. Journal of Geophysical Research, 108(B4/2217), pp.1-24

Papaioannou, Ch., (1984). Attenuation of seismic intensities and seismic hazard in the area of Greece. Ph.D. Thesis, University of Thessaloniki, 200pp.

Papanastassiou, D. (1999). Seismic hazard assessment in the area of Mystras-Sparta, south Peloponnesus, Greece, based on local seismotectonic, seismic, geologic information and on different models of rupture propagation. Natural Hazards 18, 237-251.

Papanikolaou, I.D., (2003). Generation of high resolution seismic hazard maps through integration of earthquake geology, fault mechanics theory and GIS techniques in extensional tectonic settings. Unpublished Ph.D thesis, University of London, 437pp.

Papazachos, B. C., Papaioannou, (1997). The macroseismic field of the Balkan area. Journal of Seismology 1, 181-201.

Papazachos B. C. and Papazachou C., (1997). *The earthquakes of Greece*. Thessaloniki: Ziti Publications.

Pope, R.J., Wilkinson, K.N., and Millington, A.C. (2003). Human and climatic impact on Late Quaternary deposition in the Sparta basin piedmont: Evidence from alluvial fan systems. Geoarcheology: An International Journal 18, 685-724.

Psonis, K., Latsoudas, C., (1983). 1:50000 Geological Map "Xirokampion", IGME.

Psonis, K., (1990). 1:50000 Geological Map "Sparti", IGME.

Roberts, G.P., Cowie, P., Papanikolaou, I., and Michetti, A.M., (2004). Fault scaling relationships, deformation rates and seismic hazards: An example from the Lazio-Abruzzo Apennines, central Italy. Journal of Structural Geology 26, 377-398.

Theodoulidis, N.P. (1991). Contribution to the study of strong motion in Greece. Ph.D. Thesis, University of Thessaloniki, 500pp.

Whipple, K.X., Tucker, G.E., (2002). Implications of sediment-flux-dependent river incision models for landscape evolution. Journal of Geophysical Research, 107(B2), pp.1-20.

Whittaker, A.C., Attal, M., Cowie, P.A., Tucker, G.E. & Roberts, G., (2008). Decoding temporal and spatial patterns of fault uplift using transient river long profiles. Geomorphology 100, 506-526.

Working Group on California Earthquake Probabilities, (2002). Earthquake probabilities in the San Francisco bay region: 2002-2031. USGS Open-File Report 03-214.

Wells, D.L., Coppersmith, K. (1994). New Empirical Relationships among Magnitude, Rupture Length, Rupture Width, Rupture Area, and Surface Displacement. Bull. Seismological Society of America 84, 974-1002.

Zindros, G., Exindavelonis, P. (2002). 1:50000 Geological Map "Kollinae", IGME.